

LNF-06/ 07 (P)  
February 24, 2006

## DETECTION OF PULSED SYNCHROTRON RADIATION EMISSION WITH UNCOOLED INFRARED DETECTORS

Alessio Bocci<sup>1,2</sup>, Massimo Piccinini<sup>1,3</sup>, Alessandro Drago<sup>1</sup>, Mariangela Cestelli<sup>1</sup>, Diego Sali<sup>4</sup>,  
Pierangelo Morini<sup>4</sup>, Emanuele Pace<sup>2,5</sup>, Jozef Piotrowski<sup>6</sup>, Augusto Marcelli<sup>1</sup>

<sup>1</sup>) *INFN-Laboratori Nazionali di Frascati, Via E. Fermi 40, 00044 Frascati, Italy*

<sup>2</sup>) *Università degli Studi di Firenze, Dipartimento di Astronomia e Scienza dello Spazio,  
L.go E. Fermi 2, 50125 Firenze, Italy*

<sup>3</sup>) *Università Roma Tre, Dipartimento Scienze Geologiche, L.go S. Leonardo Murialdo  
1, 00146 Roma, Italy*

<sup>4</sup>) *BRUKER Optics s.r.l., Via Pascoli 70/3, 20133 Milano, Italy*

<sup>5</sup>) *INFN, Sezione di Firenze, Via G. Sansone 11, 50019 Sesto Fiorentino (FI), Italy*

<sup>6</sup>) *VIGO SYSTEM SA, 3 Swietlikow Str., 01-389 Warsaw, Poland*

### Abstract

The synchrotron light emission is a non-thermal radiation source covering a large energy domain from IR to X-ray energies, with a time structure determined by the length and shape of the stored bunches. With suitable infrared detectors, the pulsed emission can be used to perform spectroscopic experiments at high time and spatial resolution. However, fast infrared detectors can be also applied to investigate the physical structure of the stored particles. We present here the first characterization of the synchrotron light emission at DAΦNE using detectors optimized in the mid-IR domain with a sub-ns time resolution. Experiments have been performed using the infrared SINBAD beamline, characterizing the emission of the 105 bunches stored in the electron ring of this  $e^+e^-$  collider. With both uncooled photoconductive and photovoltaic infrared detectors optimized to work at a wavelength of 10.6  $\mu\text{m}$  we resolved the infrared temporal emission of the electron bunches structure at DAΦNE characterized by bunches separated of 2.7 ns with a rise time of 176 ps and a fall time of 660 ps.

## INTRODUCTION

In the last decade both technological advances in the development of infrared detectors and their declassification for civil use made available to scientists new powerful systems for many industrial and scientific applications. Many research areas such as Astronomy, Biology, Geology, Space Applications etc., utilize these devices to perform challenging experiments just a few years ago considered impossible with the previous infrared detectors <sup>1), 2), 3)</sup>.

The infrared region is a very large wavelength range: from approximately 1  $\mu\text{m}$  to about 1000  $\mu\text{m}$ , a region that is typically divided in four energy domains: nIR (1-5  $\mu\text{m}$ ), midIR (5-20  $\mu\text{m}$ ), farIR (20-200  $\mu\text{m}$ ) and sub-millimeter and millimeter wavelengths (200-1000  $\mu\text{m}$ ). To cover this energy domain we used both quantum and thermal detectors <sup>4)</sup>. Quantum detectors based on photoconductive or photovoltaic effects may detect the energy of a single IR photon. They can be realized with intrinsic or extrinsic semiconductors with variable band gap to select the cut-off wavelengths and the detection band. Thermal detectors can detect photons from the UV down to very low energy in the extreme IR. Typical detectors for these energies are bolometers that consist of an absorber and a semiconductor or a superconductor thermometer. One of the main requirements of infrared detectors, in order to suppress the thermal generation noise, is the operation at cryogenic temperatures (i.e., 4.2 K or 77 K) that allow achieving the highest sensitivity limited by the quantum noise of the signal or background radiation. Recently, new technological capabilities allowed the development of uncooled infrared detectors, optimized to detect nIR and midIR wavelengths <sup>5)</sup>. These uncooled detectors may efficiently work with brilliant sources as quantum cascade lasers or storage ring sources such as synchrotron radiation (SR) dedicated machines or electron-positron colliders like DAΦNE <sup>6)</sup>.

DAΦNE is an  $e^+/e^-$  collider, with a center of mass energy of 1.02 GeV designed to operate with a high current and up to 120 bunches ( $\sim 20$  mA/bunch) <sup>7)</sup>. Presently, DAΦNE operates by filling 105 consecutive electron buckets out of the available 120, with a gap of 15 bunches to avoid ion trapping in the electron beam. In this bunch configuration, the minimum bunch distance is 2.7 ns and the maximum single-bunch current is  $\sim 20$  mA. The emitted light is pulsed with a time structure that depends by the filling scheme while each bunch, supposed identical, is characterized by a quasi-Gaussian shape and a length in the range 100 - 300 ps FWHM.

Since 2001 at DAΦNE is operational an infrared synchrotron radiation beamline: SINBAD (Synchrotron Infrared Beamline At DAΦNE) an apparatus dedicated to Infrared Interferometry and Microscopy <sup>8)</sup>. It collects the radiation emitted by one of the DAΦNE bending magnets at wavelengths from about 10 to 10000  $\text{cm}^{-1}$  (1-100 micron). At the end of the beamline, a microscope and a Rock-solid <sup>PM</sup> interferometer, working in a customized vacuum chamber, have been available since autumn 2002 for spectroscopy and micro-spectroscopy experiments.

Typically, nIR and midIR interferometers are equipped with single element cooled HgCdTe or InSb detectors. However, the continuous advances in infrared detectors manufacturing, pushed by military applications, have recently made new infrared array

detectors available to scientific applications, allowing very high spatial resolution at fast rate. Actually, they allow the acquisition of many spectra with a single exposition of hundreds or thousands of pixels reducing the acquisition time with respect to that required by a single element detector<sup>9) 10)</sup>. However, the time resolution of these detectors is still quite low ( $\sim 1$  ms) considering the dynamics of many physical systems so that, the availability of fast infrared detectors with ns or sub-ns response time and with faster readout time (i.e.  $\sim \mu$ s) is strategic for spectroscopic applications. Time-resolved experiments carried out using Fourier Transform Infrared (FTIR) interferometers allow to study the rich molecular structure in the midIR spectra and the fast time scale of vibrational motions with the use of Rapid and ultrarapid Scan ( $1 - 10^{-3}$  s) methods or in the case of repetitive phenomena with the Step Scan method down to  $10^{-9}$  s. These tools can probe and characterize protein folding, photo-cycles, reaction kinematics, excited electronic-state, electronic structures, as well as many dynamic chemical phenomena<sup>11)</sup>.

In principle the pulsed structure of synchrotron radiation allows to perform time-resolved experiments with resolution smaller than  $\mu$ s down to the ps domain. Indeed, in a storage ring, the typical temporal distance between two electron bunches with a length of a few hundred of picoseconds, has a value of a few nanoseconds. With such structure, these radiation sources are tools suitable to perform time resolved experiments. However these experiments require extremely fast detectors, e.g., devices that have to be characterized by high speeds, suitable to perform also diagnostic at third generation synchrotron radiation sources and at Free Electron Lasers, to detect instabilities of the stored particles and/or to measure the lengths of the accumulated bunches.

While many X-ray detectors are really fast devices, the actual technology of infrared detectors in the near and mid infrared range based on photoconductive or photovoltaic devices, cooled at liquid nitrogen temperatures, is limited to a ns response time. However, the new uncooled mid-IR range IR devices with sub-nanosecond response time can be used for fast detection of intense IR sources such as synchrotron radiation storage rings. This technology is in rapid and continuous evolution and better performances both in detectivity and in response times are expected<sup>12)</sup>. Some of these detectors are already applied to detect very fast and intense sources<sup>13), 14)</sup> or in spectroscopy applications<sup>15)</sup>.

These detectors should be also used to monitor the emission of storage ring, an application that typically requires time resolution in the ns-ps range. The experiments below described open the way to realize new diagnostic methods in storage rings and should be also used to monitor source instabilities and bunch dynamics in accelerators.

## **2 THE TIME STRUCTURE OF THE INFRARED EMISSION AT DAΦNE**

### **Measurements description and results**

At DAΦNE a series of measurements with different single element uncooled photon detectors have been performed to detect and resolve the pulsed structure at DAΦNE observing the emission at infrared wavelengths at the end of the SINBAD

beamline. We present and discuss here a set of data collected with experiments carried out with different detector configurations.

All infrared detectors have been placed at the focus of the last toroidal mirror at the end of the SINBAD beamline at the entrance of the interferometer. Different detectors have been tested with and without amplifiers, however, in the next we will present the data of two different infrared uncooled photon detectors which have been able to resolve the emission of the synchrotron radiation at DAΦNE.

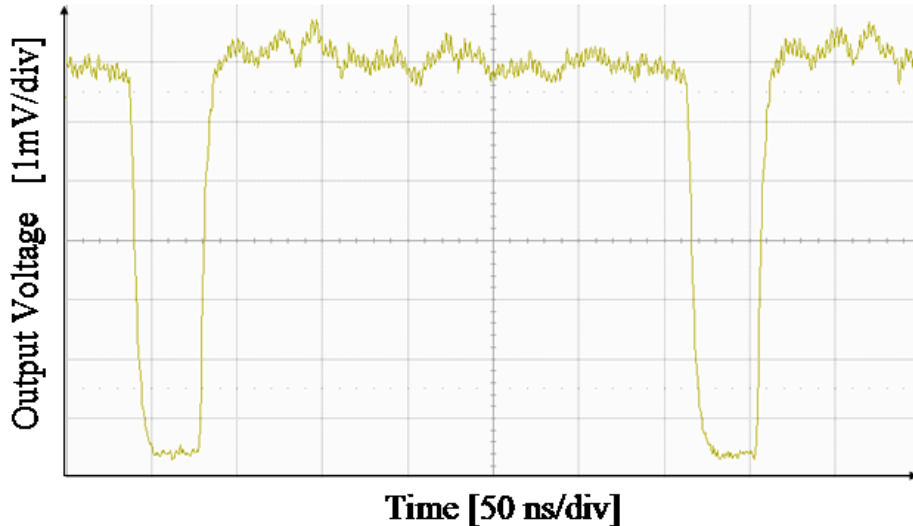
The first data refer to measurements of the IR emission of 105 bunches using a single element uncooled detector manufactured by VIGO System. This photovoltaic detector<sup>16)</sup> – series *PVMI-10.6* – (photovoltaic multiple junction detectors optically immersed) – operates at room temperature and it is characterized by a ns response time in the 8 to 12  $\mu\text{m}$  range with an optimized sensitivity at 10.6  $\mu\text{m}$ . Its multiple heterojunction photovoltaic structure is constituted by a variable gap (Hg,Cd,Zn)Te semiconductor optically immersed in a high refractive index GaAs (or CdZnTe) hyperhemispherical or hemispherical lens. With this structure this device is backside illuminated. The specifications of the detector are summarized in Tab. 1. The main advantage of this fast detector is the capability to operate at room temperature and because it does not require any cooling system it is a very small and compact device. The main drawback is the detectivity typically lower by two orders of magnitude with respect to standard cooled HgCdTe photodiodes as a result of huge generation-recombination noise at room temperature<sup>17)</sup>

The experimental setup used to monitor the DAΦNE emission is briefly described below. The 1 mm<sup>2</sup> *VIGO – PVMI-10.6* detector was placed at the focus of the last toroidal mirror of the SINBAD beamline after the diamond window separating the high vacuum inside the beamline from the interferometer station working at lower vacuum pressure or at the atmospheric pressure. The SINBAD optical system demagnifies the source image by a factor 2.3 at the final focus and its size is about 1.5x2.0 mm at midIR wavelengths<sup>18)</sup>. The IR detector output voltage was amplified by a Mini-Circuits ZFL500 linear amplifier with an input impedance of 50  $\Omega$ , bandwidth of 0.05 - 500 MHz, voltage gain ( $A_v$ ) of about 20 db and Noise-Figure (NF) of 6 dB. The amplified signal was analyzed by the oscilloscope model LeCroy WaveSurfer 454 with an acquisition time of 2 Gsamples/s in a single-shot sample rate, a bandwidth of 500 MHz and a rise time of 800 ps. Detector, preamplifier and scope were connected by double shielded RG223 cables and BNC connectors. The use of RG223 cables was necessary to eliminate an unwanted high frequency background signal noise detected when single-shield RG58 were used.

**TAB. 1:** Technical characteristics of the photovoltaic IR detector<sup>7)</sup>.

<i>Detector Type</i>	<i>VIGO – PVMI-10.6</i>
Working Temperature	300 K
Responsivity (@10.6 $\mu\text{m}$ )	0.27 V W <sup>-1</sup>
Noise Density	1.3 nV Hz <sup>-1/2</sup>
Detectivity (@10.6 $\mu\text{m}$ )	$(2.1 \pm 0.4) \cdot 10^7 \text{ W}^{-1} \text{cm Hz}^{1/2}$
Detectivity (@ $\lambda_{\text{peak}}$ )	$\geq 2 \cdot 10^8 \text{ W}^{-1} \text{cm Hz}^{1/2}$
Detector Resistance	105 $\Omega$
Response Time	$\leq 1$ ns
Optical Area	1 mm x 1 mm
Bandwidth	DC to VHF
Field of view	38 degrees

This experimental setup was used to collect the emission both of the normal operation of DAΦNE and of a particular bunch structure described in the next. In the standard configuration, DAΦNE operates with a structure of 105 electron bunches equally spaced plus a time gap of 15 equivalent bunches. Because DAΦNE is an  $e^+e^-$  collider, the radio-frequency (RF) system of each ring consists of a normal conducting single cell cavity running at 368 MHz on the 120<sup>th</sup> harmonic of the revolution period. Therefore, the natural gap between two bunches is  $\sim 2.7$  ns. The observed infrared synchrotron radiation emission of the 105 electron bunches during standard operation is shown in Fig. 1.

**FIG. 1:** The signal corresponding to the radiation emitted by the 105 stored electron bunches at DAΦNE as measured by the amplified IR detector.

As shown in Fig. 1, with an average stored electron current of  $\sim 1$  A the output voltage of the IR detector amplified by a 20 dB voltage amplifier is  $\sim 6.5$  mV. The signal duration is about 285 ns that correspond exactly to the expected time length of 105 bunches, while the observed gap of about 40 ns corresponds to the time length of 15 equivalent bunches. The time scale of the signal in Fig. 1 is 325 ns, i.e., the frequency of

3.07 MHz corresponding to 120 bunches. In Fig. 1 is also evident a background, mainly associated to the signal associated to all bunches, while the signal corresponding to the gap does not show the same noise level. Fig. 1 clearly shows that in this set up the IR photovoltaic detector is not able to resolve the emission of bunches separated by a few ns, but it detect only a continuous emission.

In order to characterize the effective detector speed trying to resolve the emission of a single bunch, in a second set of measurements a particular bunch structure was selected and stored at DAΦNE. In the structure described in Fig. 2, each box of the table represents an electron bunch (from 1 to 120). The red boxes represent the bunch injected and stored in the selected structure, while the white boxes correspond to the empty bunch positions. In this way different contiguous bunch configurations can be filled and it is possible investigate different gaps and recognize the emission of a single bunch characterizing the time response of the detector.

Fig. 3 shows the IR signal measured by the detector with such configuration. The overall structure of the IR emission is well resolved according to the bunch structure described in Fig. 2.

1	2	3	4	5	6	7	8	9	10	11	12	13	14	15	16	17	18	19	20
21	22	23	24	25	26	27	28	29	30	31	32	33	34	35	36	37	38	39	40
41	42	43	44	45	46	47	48	49	50	51	52	53	54	55	56	57	58	59	60
61	62	63	64	65	66	67	68	69	70	71	72	73	74	75	76	77	78	79	80
81	82	83	84	85	86	87	88	89	90	91	92	93	94	95	96	97	98	99	100
101	102	103	104	105	106	107	108	109	110	111	112	113	114	115	116	117	118	119	120

**FIG. 2:** Configuration of the DAΦNE bunches selected in order to characterize the detector speed and to resolve the IR emission of a single electron bunch.

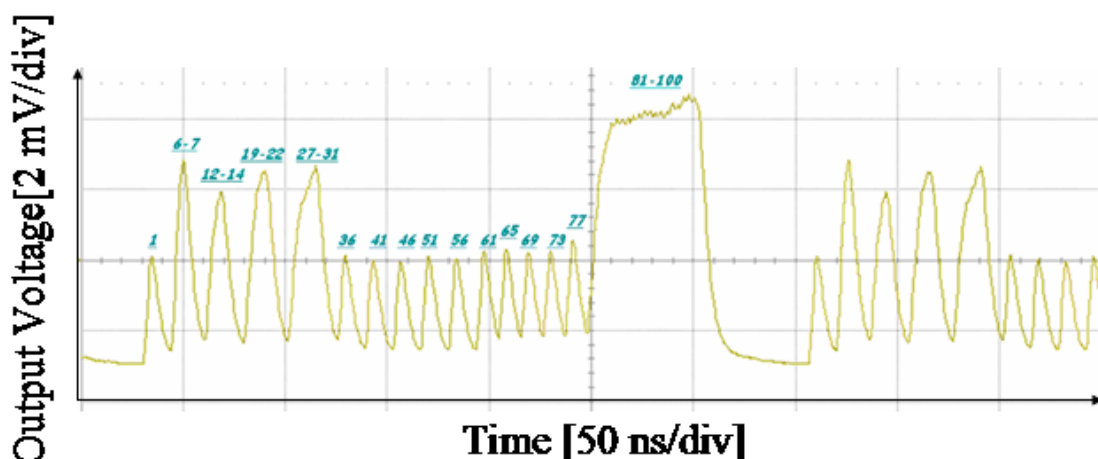


**FIG. 3:** IR signal of the DAΦNE bunches structure described in Fig. 2. The x and y scales are 50 ns/div and 2mV/div respectively.

For the configuration of Fig. 2, each electron bunch was filled with a current of about 10 mA providing a total current value of 415 mA. Looking at Fig. 3, the signal associated to a single bunch is a factor of 2 or lower than the signal corresponding to the

emission of 2 (or more) consecutive bunches each one separated by 2.7 ns. From these data the resolution time of the detector is not able to discriminate the emission of two bunches separated by 2.7 ns while it allows to separate the emission of individual bunches only when the gap is not smaller than 10.8 ns e.g., the length equivalent to 3 bunches (see the emission among bunches from 61 to 77 in Fig. 3).

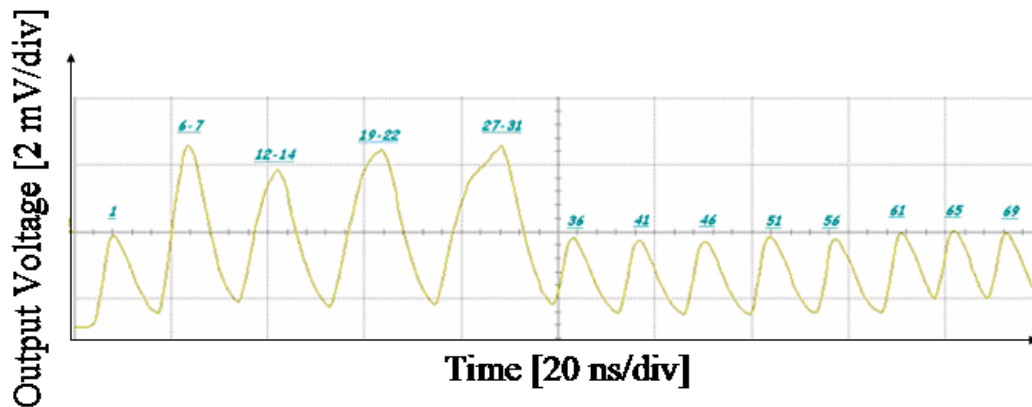


**FIG. 4:** A zoomed view of the IR emission of the bunch structure described in Fig. 2.

The gap between the emission of the electron bunches is clearly visible in Fig. 4 where the signal associated to this bunch structure up to the bunch number 69 has been plotted in an expanded scale. The gap between the emission of stored electron bunches ranging from 36 to 61 is  $\sim 13$  ns while that of those ranging from 61 to 69 is  $\sim 10$  ns, as expected. Measurements also with single bunch stored in DAΦNE collider have been realized. The emission structure of one single bunch as measured by the photovoltaic detector is shown in Fig. 5. Using this signal, it was possible to evaluate the response time of the entire system of about 3.5 ns. In all the experiments described the detector was connected to the input of the preamplifier box outside the interferometer with a RG223 BNC cable with length of about of one meter. Since the response time of the detector was estimated of about 1 ns, to verify if the problems of the higher response time of the system was due by the connection with the cable successive measurements have been realized in another configuration without the BNC cable.

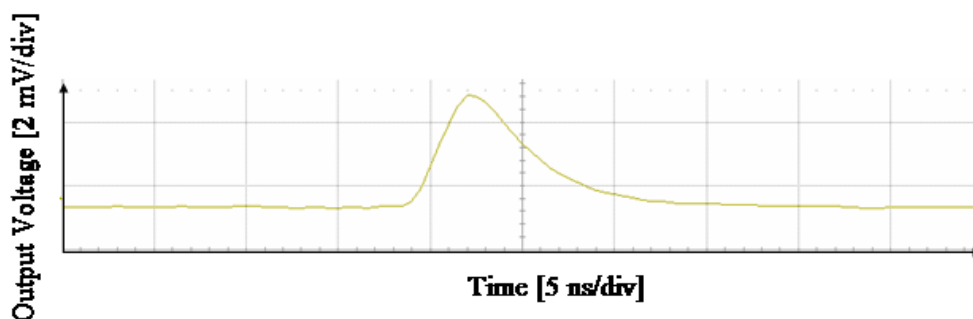


**FIG. 5:** The signal emitted by a single bunch as measured by the IR photovoltaic detector.

The results obtained in the experimental configuration that we will show in the next confirm that all the previous measurements were mainly limited by the rise time of the

BNC cable and not by the detector. So to check the result another test has been performed with the same photovoltaic detector connected without the BNC cable to a different amplifier, a Mini-Circuits ZJL-4HG medium power amplifier with an input impedance of  $50 \Omega$ , bandwidth of 20 - 4000 MHz, voltage gain ( $A_v$ ) of about 18 dB and Noise-Figure (NF) of 5 dB at 1.5 GHz. A second Mini-Circuits ZFL500 amplifier similar to that of the first measurements has been connected in series to obtain a higher output voltage signal e.g., a total gain amplification of about 38 dB. The measured signal, analyzed by an oscilloscope model 8000 Series Infiniium with an acquisition time of 2 Gsamples/s, a bandwidth of 600 MHz and a rise time of 583 ps is shown in Fig. 6.

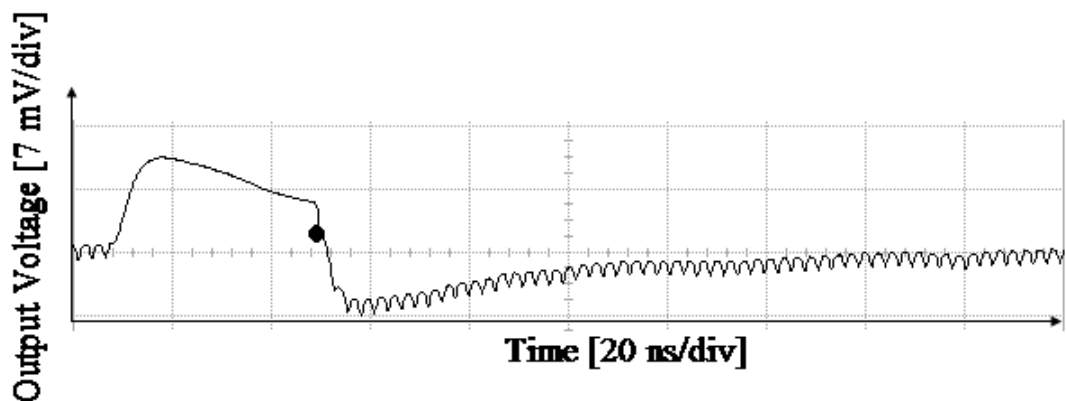


**FIG. 6:** The IR signal emitted by the DAΦNE bunches and the gap as measured by the photovoltaic detector with a different amplification set-up. The IR signal is negative because of the configuration of one of the two amplifiers used.

This second set of measurements have been performed with the photovoltaic detector and DAΦNE working in normal condition, e.g., with 105 consecutive buckets filled and a maximum stored current of 1.5 A. In Fig. 6 is clearly visible the gap and the emission signals of different electron bunches separated by 2.7 ns.

Data can be interpreted as distortion of waveforms by too long response time of detection system. This can be caused by: i) detector RC time constant, ii) long collection time of charge carriers or iii) distortion of waveforms by electronics.

i) The PVM detector is a backside illuminated multiple heterojunction photovoltaic device with complex architecture.<sup>19)</sup> It is characterized by a low junction resistance and capacitance. The RC time constant, according to computer simulations, should be significantly less than 1nsec. So it seems unlikely to determine device response time.

ii) The collection time for charge carriers generated by absorption of IR radiation in the  $10.6 \mu\text{m}$ -optimized absorber region, characterized by a short recombination lifetime, is less than the 0.6ns. But more short wavelength could be absorbed at the absorber/CdTe buffer interface. This region is characterized by more long recombination time and long collection time for charge carriers photogenerated there. Therefore, this could be a possible reason for increased response time for detection of IR beam rich in short wavelength radiation. The problem can be solved with suitable design of the device.



iii) The increase of response time could be caused by the too slow electronics.

Improved results have been obtained with a second detector, e.g. a single element uncooled photoconductive detector – series R005<sup>20)</sup>. This device is a high speed, ambient temperature photoconductive IR detector again optimized at 10.6  $\mu\text{m}$  and realized with a quaternary Hg-Cd-Zn-Te semiconductor. This device is front-side illuminated so the absorption of any wavelength radiation occurs only in the narrow gap absorber characterized by a short recombination time. The main parameters of the detector are summarized in Tab. 2.

**TAB. 2:** Technical characteristics of the photoconductive IR detector

<i>Detector Type</i>	<i>VIGO – R005–3</i>
Working Temperature	300 K
Responsivity (@10.6 $\mu\text{m}$ )	$> 0.05 \text{ V W}^{-1}$
Detectivity (@10.6 $\mu\text{m}$ )	$> 3 \cdot 10^6 \text{ W}^{-1} \text{ cm Hz}^{1/2}$
Detectivity (@ $\lambda_{\text{peak}}$ )	$> 8 \cdot 10^6 \text{ W}^{-1} \text{ cm Hz}^{1/2}$
Detector Resistance	50 – 80 $\Omega$
Response Time	$< 1 \text{ ns}$
Optical Area	1 mm x 1 mm
1/f corner frequency	10 – 100 kHz
Field of View	$> 60 \text{ degrees}$

The measurements have been performed biasing the detector with a current of about 20 mA with a Bias Tee model MiniCircuits ZFBT-4R2G in a modified configuration connecting in series to the DC input of the Bias Tee a resistance of 500  $\Omega$ . The bandwidth of the bias tee was 10-4200 MHz. The signal at the output has been amplified with the same configuration previously described with the two amplifiers connected in series. The amplified signal was analyzed by an oscilloscope model Tektronix TDS 820 with an acquisition time of 66.66 ksamples/s, a bandwidth of 6 GHz and a rise time of 58.3 ps. In the Figures 7 and 8 we show the IR emission measured with this set-up. While data in Fig. 7 refer to an average of about 1000 acquisition the data shown in Fig. 8 represent only two data acquisitions.

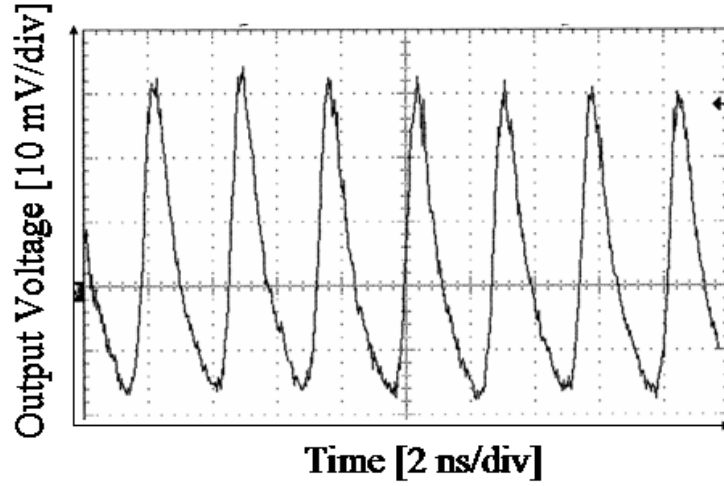


**FIG. 7:** The IR emission of the DAΦNE bunches as measured by the photoconductive detector (1000 acquisitions).

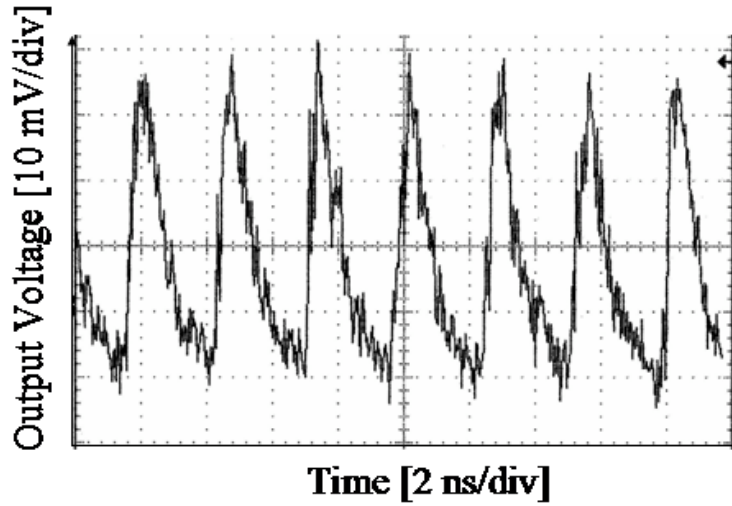


**FIG. 8:** IR signal of some DAΦNE bunches measured with the photoconductive detector (2 acquisitions).

For the configuration described above the minimum measured rise time and fall time of the signal emitted by a single electron bunch are 296 ps and 1.092 ns respectively for the data of Fig. 7 and 176 ps and 660 ps respectively for the data of Fig. 8. The response time  $\tau$  of the detector, defined as the time that the detector takes to reach the  $1/e$  value of the initial one after the irradiation is switched off has been evaluated using the equation<sup>20)</sup>:

$$t_f^{10-90} = 2.19 \tau \quad (1)$$

where  $t_f^{10-90}$  is the fall time of the detector, defined as the time that the output signal of the detector goes from 90% to 10% of its final value.

The estimated response time  $\tau$  is  $\sim 500$  ps, e.g., equivalent to a bandwidth of 318 MHz for the data of Fig. 7 and  $\tau \sim 300$  ps, e.g., equivalent to a bandwidth of 530 MHz for the data of Fig. 8. In the second case the lower response time is probably due to the limited numbers of acquisitions.

These results clearly show that the characterization of the time structure of the storage ring emission at IR wavelengths is nowadays possible. Other systems and faster configurations are under test but already with these devices we were able to resolve in the infrared region a single bunch emission and we expect to resolve the shape of a single bunch emission at DAΦNE. While these experiments allow a complete characterization of fast detector devices, they also show that the detection of storage ring emission is feasible.

## Conclusions

We report a series of experiments characterizing the performances of uncooled fast IR detectors using the pulsed synchrotron radiation emission of the DAΦNE storage ring. These experimental data represent also the first direct measurement of the midIR light emission of electron bunches using an uncooled fast IR detector with a sub-ns resolution.

The best results in resolution time has been obtained with photoconductive detectors optimized to work at 10.6  $\mu\text{m}$  of wavelength and with a response time of about 300 ps. With this detector a minimum rise time of 176 ps and a minimum fall time of 600 ps have been observed. The photovoltaic detectors we tested are characterized by a lower response time that appear not yet optimized to detect the pulsed time structure of the DAΦNE collider. These measurements could be very important also to understand better the time behaviour of photovoltaic devices. Actually, much faster photovoltaic detectors can be manufactured and response time as short as 50 ps are achievable with high frequency optimized devices<sup>5), 17)</sup>.

With this detector we resolved the bunch structure at DAΦNE observing the IR emission of two consecutive stored bunches separated by about 2.7 ns. These experiments open the way to realize new diagnostic methods in storage rings and should be also used to monitor source instabilities and bunch dynamics.

Moreover, in the next future, investigation of the intrinsic emission structure of a single bunch in the mid-ir wavelengths will be possible using detectors characterized by a response time of a few ps and also arrays of these detectors should be also applied for fast imaging applications to investigate the characteristics and the dynamics of electron bunches.

## REFERENCES

- (1) P. Colarusso, L.H. Kidder, I.W. Levin, J.C. Fraser, J.E. Arens, E.N. Lewis, *Appl. Spectrosc.* **52**, 106A (1998)
- (2) A.W. Hoffman, P. J. Love, J. P. Rosbeck, *Proceedings of the SPIE*, Volume 5167, pp. 194-203 (2004)
- (3) A. Rogalski, *Rep. Prog. Phys.* **68** (2005) 2267–2336
- (4) A. Rogalski, *Quant. Electron.* **27**, 59 (2003)
- (5) J. Piotrowski, A. Rogalski, *Infrared Phys. Technol.* **46**, 115 (2004)
- (6) A. Bocci, M. Piccinini, A. Drago, D. Sali, P. Morini, E. Pace, A. Marcelli, LNF-05-12 (NT), (2005)

- (7) A. Drago, D. Alesini, G. Benedetti, M.E. Biagini, C. Biscari, R. Boni, M. Boscolo, A. Clozza, G. Delle Monache, G. Di Pirro, A. Gallo, A. Ghigo, S. Guiducci, F. Marcellini, G. Mazzitelli, C. Milardi, L. Pellegrino, M.A. Preger, P. Raimondi, R. Ricci, C. Sanelli, M. Serio, F. Sgamma, A. Stecchi, C. Vaccarezza, M. Zobov, Proc. PAC2003, Portland, Oregon, (2003)
- (8) M. Cestelli Guidi *et al.*, *Jour. Opt. Soc. Amer.* **A22**, 2810 (2005).
- (9) I. W. Levin, R. Bhargava, *Appl. Spectrosc.*, *Annual Rev. Phys. Chem.* 56, 429 (2005)
- (10) A. Bocci, E. Pace, A. Marcelli, P. Morini, D. Sali, Proceedings of the 9th ICATPP Conference on Astroparticle, Particle, Space Physics, Detectors and Medical Physics Applications , Villa, Olmo, Como, Italy 17-21 October 2005, in press.
- (11) G. D. Smith, R A Palmer, *Handbook of Vibrational Spectroscopy* **1**, 625 (2002)
- (12) A. Piotrowski *et al.*, *Bull. Pol. Acad. Sci., Tech. Sci.* **53**, 139 (2005).
- (13) G.S. Edwards, R.H. Austin, F.E. Carroll, M.L. Copeland, M.E. Couprie, W.E.Gabella, R.F. Haglund, B.A. Hooper, M.S. Hutson, E.D. Jansen, K.M. Joos, D.P. Kiehart, I. Lindau, J. Miao, H.S. Pratisto, J.H. Shen, Y. Tokutake, L. van der Meer and Aihua Xie, *Rev. Sci. Instru.* **74**, 3207-3245 (2003).
- (14) D. Hofstetter, M. Beck, T. Aellen, and S. Blaser, *IEEE Photon. Technol. Lett.* **15**, 1044 (2003).
- (15) L. Menzel, A.A. Kosterev, R.F.Curl, F.K. Tittel, C.Gmachl, F. Capasso, D.L. Sivco, J.N. Baillargeon, A.L. Hutchinson, A.Y.Cho, W.Urban, *Appl. Phys. B* **72**, 859–863 (2001).
- (16) <http://www.vigo.com.pl/dane/detektory/pvmi.pdf>.
- (17) J. Piotrowski, *Opto-Electron. Rev.* **12**, 111 (2004).
- (18) M. Cestelli Guidi, A. Marcelli, A. Nucara and P. Calvani, LNF Report,04/004 (IR).
- (19) J. Piotrowski, Z. Nowak, J. Antoszewski, C. Musca, , J. Dell, and L. Faraone, *Semicond. Sci. Technol.* **13**, 1209-1214 (1998).
- (20) <http://www.vigo.com.pl/dane/detektory/pc.pdf>.
- (21) E.L. Dereniak, D.G. Crowe, *Optical Radiation Detectors*, Appendix D, 551, (1984).